A Comparative Study on the Effects of 5-(3-Aminophenyl)-tetrazole on the Inhibition of Magnesium Corrosion in Natural Seawater and 3.5 wt.% NaCl Solutions

El-Sayed M. Sherif [1,2,*]

[1] Center of Excellence for Research in Engineering Materials (CEREM), College of Engineering, King Saud University, P. O. Box 800, Al-Riyadh 11421, Saudi Arabia
[2] Electrochemistry and Corrosion Laboratory, Department of Physical Chemistry, National Research Centre (NRC), Dokki, 12622 Cairo, Egypt
E-mail: esherif@ksu.edu.sa

In the present work, the effects of 5-(3-aminophenyl)-tetrazole (APTA) on the corrosion inhibition of magnesium in Arabian Gulf seawater (AGS) and 3.5 wt.% NaCl solutions were reported. Different experimental techniques namely, weight-loss (WtL), potentiodynamic polarization (PDP), potentiostatic current-time (CCT), electrochemical impedance spectroscopy (EIS), and scanning electron microscopy (SEM) with X-ray analyzer (EDX) were employed. It has been found that AGS has almost similar effect compared to 3.5 wt.% NaCl on Mg uniform corrosion but it has higher effect on the Mg pitting and microbial induced corrosion than NaCl has. The presence of 1×10^{-3} M APTA and the increase of its concentration to 5×10^{-3} M highly reduce the corrosion of Mg in both AGS and NaCl solutions. This was confirmed by the decrease of corrosion current and corrosion rate as well as the increase of surface and polarization resistances for Mg after its immersion in AGS and NaCl containing APTA molecules. The surface morphology obtained by SEM and profile analysis acquired by EDX stated that the surface of Mg is compacted and protected in the presence of APTA molecules.

1. INTRODUCTION

Magnesium is an important engineering material because of its light weight and excellent properties. Its density is 1.74 g·cm^{-3}, only 2/3 that of aluminum and 1/4 that of iron. In addition, Mg and its alloys are characterized by good electro-magnetic shield, and excellent damping and heat

dissipation. Therefore, Mg and its alloys have been greatly used in aerospace constructions, aircraft, automotive, manufacturing of mobile phones, laptop computers, biomaterials, cameras, and other electronic components [1-7]. Mg itself is a very reactive metal and once produced, it is coated in a thin layer of its oxide because of which, its free element is not naturally found on earth. This layer is not combined and compact enough to provide full protection for Mg against corrosion, especially in salty water like seawater and chloride containing environments [1,3]. The Cl⁻ ions from the surrounding environment penetrate the oxide layer to reach then react with the surface of Mg, which leads to its severe corrosion [8-12].

The high corrosion susceptibility of Mg is also expected due to its high negative potential that makes it very reactive with the surrounding media. It has been also reported [13,14] that if the Mg alloys have impurities and second phases within their structures, these will be considered as active cathodic sites, which will accelerate the local galvanic corrosion of the alloy matrix. The presence of impurities such as iron, copper and nickel in low amounts increases the corrosion resistant of the Mg alloy. These elements if present in high contents will act as active cathodes with small hydrogen overvoltage and result in dissolution of the Mg matrix [15-17]. Therefore, the corrosion and corrosion protection of Mg in different aggressive environments have been reported by several investigators [8-12, 18,19].

Corrosion inhibitors have been reported [20-32] to be one of the most important methods for the protection of different metals and alloys against corrosion in harsh environments. Although, a great number of investigations have been devoted to the protection of magnesium, very little work has been seldom involved on the adding corrosion inhibitors [1,3,33-35]. The outcome of these studies reported that the organic compounds that can form an inhibitor-magnesium precipitation in aqueous solution could be used as corrosion inhibitors for magnesium alloys to inhibit the increase of polarization current density as well as the dissolution and oxidation of magnesium alloys effectively [1,3,33-35].

The objective of the current work was to report the effect of 5-(3-aminophenyl)-tetrazole (APTA) on the inhibition of magnesium corrosion after 60 min immersion in Arabian Gulf seawater and 3.5 wt.% sodium chloride solutions. This compound, APTA, has been reported to show excellent performance as a corrosion inhibitor for copper [36, 37] and iron [38] in chloride media. To achieve the proposed objective, weight-loss, potentiodynamic polarization, chronoamperometric current-time at constant potential and electrochemical impedance spectroscopy measurements were used. The work was also complemented using scanning electron microscope and energy dispersive X-ray investigations.

2. EXPERIMENTAL PROCEDURE

Natural Arabian Gulf seawater (AGS) was obtained from the Arabian Gulf at the eastern region (Dammam, Jubail, Saudi Arabia), sodium chloride (NaCl, Merck, 99%), 5-(3-Aminophenyl)-tetrazole (APT, Alfa-Aesar, 96%), and absolute ethanol (C_2H_5OH, Merck, 99.9%) were used as received. An electrochemical cell with a three-electrode configuration was used; a Mg-07%Mn rod having 1.2 cm side length and total surface of 1.44 cm^2, a platinum foil, and an Ag/AgCl electrode (in a saturated

KCl) were used as the working, counter, and reference electrodes, respectively. The Mg rod for electrochemical measurements was prepared by welding a copper wire to a drilled hole was made on one face of the rod; the rod with the attached wire were then cold mounted in resin and left to dry in air for 24 h at room temperature. Before measurements, the free face of the Mg electrode, which was not drilled and not covered with the epoxy resin, was polished successively with metallographic emery paper of increasing fineness up to 1200 grit. The electrode was then cleaned using doubly-distilled water, degreased with acetone, washed using doubly-distilled water again and finally dried with a stream of dry air. In order to prevent the possibility of crevice corrosion during measurement, the interface between sample and resin was coated with Bostik Quickset, a polyacrelate resin.

The weight-loss experiments were carried out using rectangular magnesium coupons having a dimension of 4.0 cm length, 2.0 cm width and 0.4 cm thickness. The coupons were polished and dried as for the case of Mg rods, weighed, and then suspended in 300 cm^3 solutions of AGS and 3.5 wt.% NaCl solutions in the absence and the presence of 1×10^{-3} M and 5×10^{-3} M APTA for varied exposure periods from 120 to 600 hours. The values of the loss in weight per area (Δm, mg cm^{-2}), the corrosion rate (K_{Corr}, mg cm^{-2} h^{-1}), and the percentage of the inhibition efficiency (IE%) for Mg coupons in the test solutions were calculated according to the following relations [39-43],

$$\Delta m = \frac{m_{int} - m_{fin}}{A} \tag{1}$$

$$K_{Corr} = \frac{m_{int} - m_{fin}}{A\ t} \tag{2}$$

$$IE\% = 100 \left(\frac{K_{Corr}^{un} - K_{Corr}^{Inh}}{K_{Corr}^{un}} \right) \tag{3}$$

Where, m_{int} is the initial weight (mg) before immersion, m_{fin} is the final weight (mg) after exposure to the test solution, A is the total surface area, 54.0 cm^2, t is the time of exposure in hours, K_{Corr}^{un} is the corrosion rate of Mg in the test solutions that did not have APTA molecules, and K_{Corr}^{inh} is the corrosion rate of Mg coupons in the test solutions that contained APTA molecules.

The SEM investigation and EDX analysis were obtained for the surface of magnesium specimens after their immersions for 600 hours in AGS and 3.5 wt.% NaCl solutions in absence and presence APTA molecules. The SEM micrographs and EDX profile spectra were collected by using a JEOL model JSM-6610LV (Japanese made) scanning electron microscope having an energy dispersive X-ray analyzer attached.

Electrochemical experiments were performed by using an Autolab Potentiostat (PGSTAT20 computer controlled) operated by the general purpose electrochemical software (GPES) version 4.9. The polarization curves were obtained by scanning the potential in the forward direction from -2000 to -800 mV against Ag/AgCl at a scan rate of 3.0mV/s. Chronoamperometric measurements at constant anodic potential were carried out by stepping the potential of the magnesium rods to −1200 mV versus Ag/AgCl. Electrochemical impedance spectroscopy data were obtained at corrosion potential over a

frequency range from 100000 Hz to 0.1Hz, with an ac wave of ± 5 mV peak-to-peak overlaid on a dc bias potential, and the impedance spectra were collected using Powersine software at a rate of 10 points per decade change in frequency. All electrochemical experiments were performed at room temperature in naturally aerated solutions and the data were collected after Mg immersion for 60 min.

3. RESULTS AND DISCUSSION

3. 1. Weight-loss data, SEM / EDX investigations and inhibition efficiency

Figure 1 shows the weight loss (Δm / mg.cm^{-2}) time (t / h) relationship for Mg coupons in aerated solutions of (a) AGS and (b) 3.5 wt.% NaCl in the absence of APTA (1) and the presence of 1×10^{-3} M APTA (2) and 5×10^{-3} M APTA (3), respectively. It is clearly seen from Fig. 1 (curves 1) that the loss in Mg weight increased with increasing the immersion time in AGS and NaCl in the absence of APTA molecules. This is due to the continuous dissolution of Mg as a result of the corrosive ions attack of the media under investigation. The anodic reaction that causes this dissolution, which occurs upon immersing Mg in the solution as follows [44];
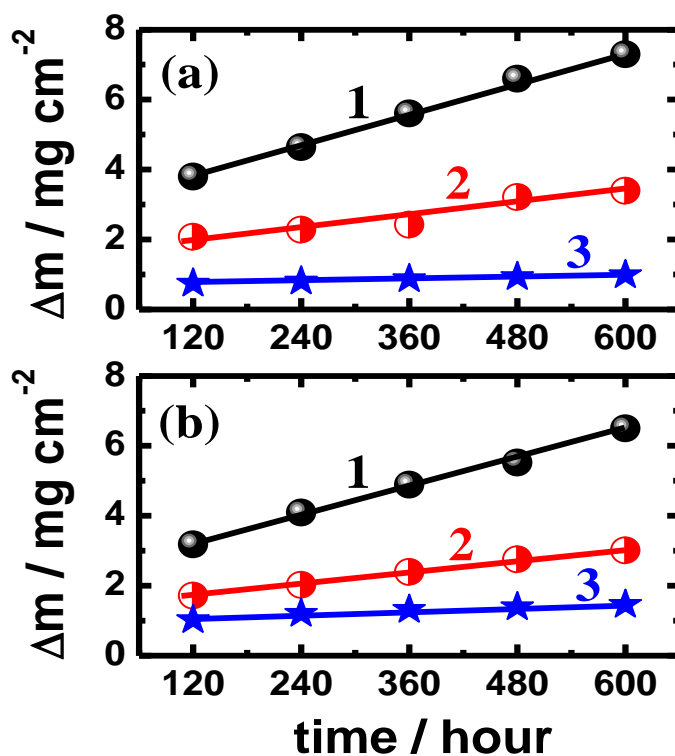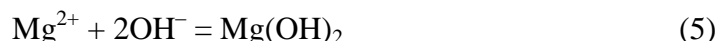
$$Mg = Mg^{2+} + 2e^{-} \tag{4}$$

Figure 1. The variation of weight-loss (Δm / mg cm^{-2}) as a function of time (hour) for Mg coupons in (a) AGS and (b) 3.5 wt.% NaCl solutions that contain (1) 0.0 M APTA, (2) 1.0×10^{-3} M APTA, and (3) 5.0×10^{-3} M APTA, respectively.

These magnesium cations then react with the hydroxide ions to form magnesium hydroxide as follows;

$$Mg^{2+} + 2OH^- = Mg(OH)_2 \qquad (5)$$

The hydroxide ions here were produced due to the occurrence of a disturbed equilibrium between the water of the test solution and its ions, which leads to a stronger reaction in the forward direction [45];

$$H_2O = (OH^-)_{Mg} + H^+ \qquad (6)$$

The cathodic reaction for Mg at this conditions has been reported to be the hydrogen evolution [45]; unlike other metals and alloys, for which the cathodic reaction in seawater and sodium chloride solutions, is the oxygen reduction. This also occurs because the electron consumption on magnesium happens by the unloading of hydrogen ions (acidic corrosion) according to the following equation [45],

$$2H^+ + 2e^- = H_2 \qquad (7)$$

The occurrence of this strong reaction leads to a strong anodic dissolution reaction for Mg and thus leads to the linear increase in the weight loss with time as indicated by curves 1 of Fig. 1.

The presence of APTA, 1×10^{-3} M in the seawater, Fig. 1a, curve 2, significantly decreased the weight loss over the whole time of Mg exposure. This effect is further increased when the concentration of APTA increased to 5×10^{-3} M as can be seen from curve 3 of Fig. 1a. The effect of APTA on the values of Δm for Mg in NaCl solutions, Fig. 1b, curve 2 and curve 3, was almost similar to that in the AGS ones at the same concentration. It is clearly seen from Fig. 1 also that although, the dissolution of Mg in AGS was noticeably higher than in NaCl solution, the dissolution of Mg in AGS in the presence of APTA and the increase of its content was lower than in case of NaCl solutions.

The change of corrosion rate (K_{Corr} / mg cm^{-2} h^{-1}) as a function of time (hour) for Mg coupons in (a) AGS and (b) 3.5 wt.% NaCl solutions that contain (1) 0.0 M APTA, (2) 1.0×10^{-3} M APTA, and (3) 5.0×10^{-3} M APTA, respectively is shown in Fig. 2. The K_{Corr} for Mg in either AGS or NaCl solution in the absence of APTA recorded the highest values, which resulted from the aggressiveness nature of these media toward Mg. It is seen also that these K_{Corr} values decrease with the increase of immersion time. This occurs because the corrosion occurs faster for fresh Mg surfaces. The corroded surfaces then develop layers of corrosion products and/or oxide films, which in turn cover up the surface and lead to decreasing the uniform corrosion of Mg with time. This includes the formation of $Mg(OH)_2$ as shown by Eq. (5) and an Mg oxide film according to [44-46];

$$Mg + O = MgO \qquad (8)$$

The presence of APTA molecules either with AGS or NaCl solutions decreased the values of K_{Corr} over the whole time of the measurements and this effect increased with increasing the

concentration of APTA from $1x10^{-3}$ to $5x10^{-3}$ M. The protection of Mg surface by the APTA molecules is apparently the due to the protective action of APT molecules.
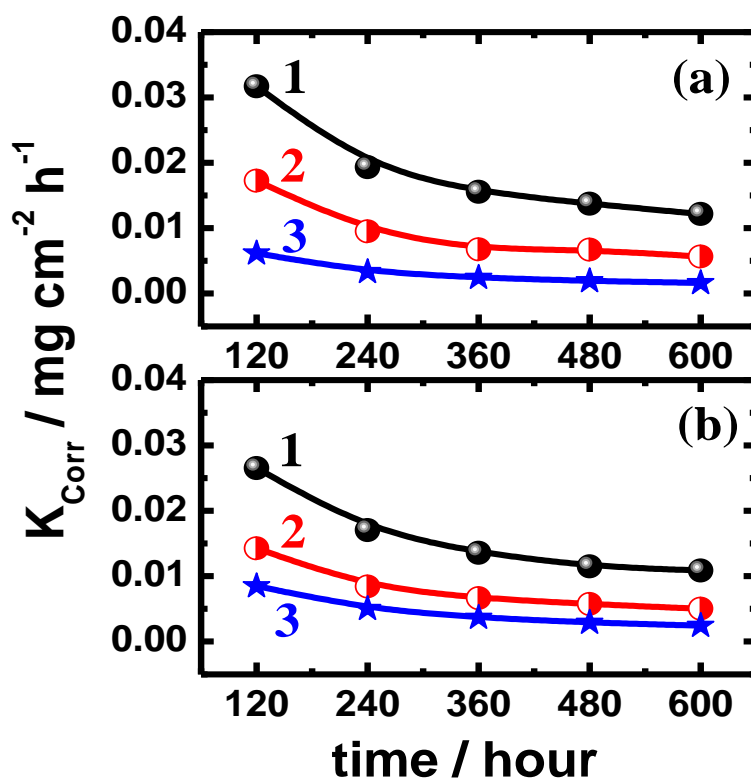

Figure 2. The change of corrosion rate (K_{Corr} / mg cm^{-2} h^{-1}) as a function of time (hour) for Mg coupons in (a) AGS and (b) 3.5 wt.% NaCl solutions that contain (1) 0.0 M APTA, (2) $1.0x10^{-3}$ M APTA, and (3) $5.0x10^{-3}$ M APTA, respectively.

In order to differentiate between the effect of APTA on the surface morphology of Mg after its immersion for 600 h in AGS and 3.5 wt.% NaCl in absence and presence of M APTA molecules, the SEM and EDX investigations were carried out. Fig. 3 shows the SEM micrographs for Mg after its immersion for 600 hours in (a) AGS alone, and (b) AGS + $1x10^{-3}$ M APTA; the corresponding EDX profile analyses (c) and (d) are for Mg surface that shown in the micrographs (a) and (b), respectively. The SEM micrograph, Fig. 3a, shows that the surface of Mg is completely covered with corrosion product layers and there are few shaped like mushroom formed on the surface. The atomic percentages of the elements found in the area shown in the SEM micrograph as represented by the EDX profile displayed in Fig. 3c, were 62.12% O, 16.11% C, 19.06% Ca, 0.14% Sr, and only 2.58% Mg. The small amounts of Mg indicate that the investigated surface has a thick corrosion product layer, which is probably due to the presence of a certain type of micro-organisms in the seawater. On the other hand, and in the presence of APTA with the chloride solution, Fig 3b, the SEM image shows a thick and more homogenous layer covers the surface of the Mg. This layer does not show any shaped like mushrooms that were shown in Fig. 3a for Mg surface in the absence of APTA molecules. The EDX

analysis (Fig. 3d) for the selected SEM area that is shown in Fig. 3b, has given the following elemental percentage, 60.58% O, 18.80% C, 17.20% Ca, 3.12% Mg, 0.16% Sr, 0.12% S and 0.2% Na.
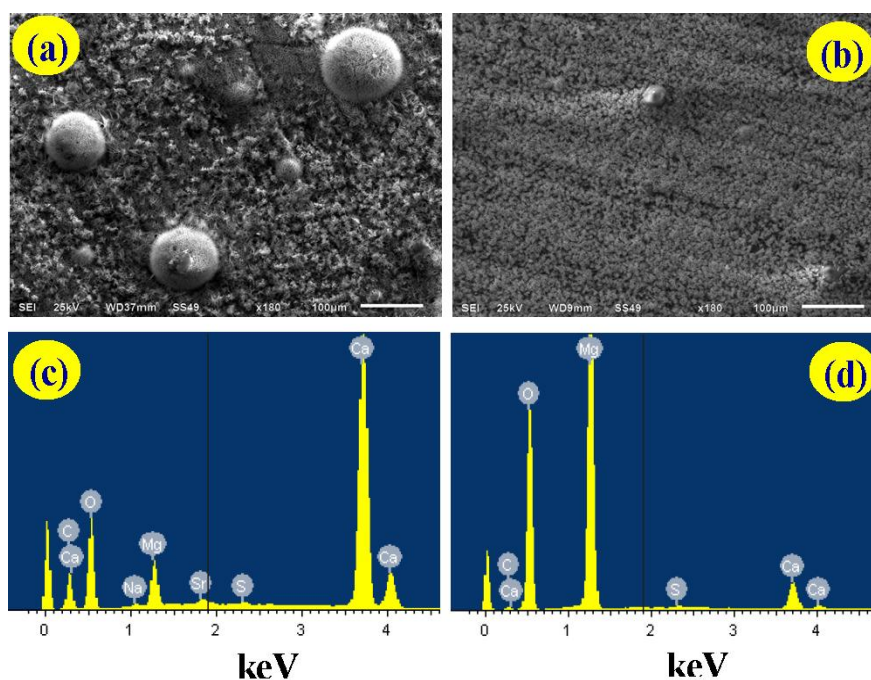

Figure 3. SEM micrograph for Mg after its immersion for 600 hours in (a) AGS alone, and (b) AGS + 1×10^{-3} M APTA; the corresponding EDX profile analysis, (c) and (d) for Mg surface shown in the micrographs (a) and (b), respectively.

Figure 4. SEM micrograph for Mg after its immersion for 600 hours in (a) 3.5 wt.% NaCl alone, and (b) 3.5 wt.% NaCl + 1×10^{-3} M APTA; the corresponding EDX profile analysis, (c) and (d) for Mg surface shown in the micrographs (a) and (b), respectively.
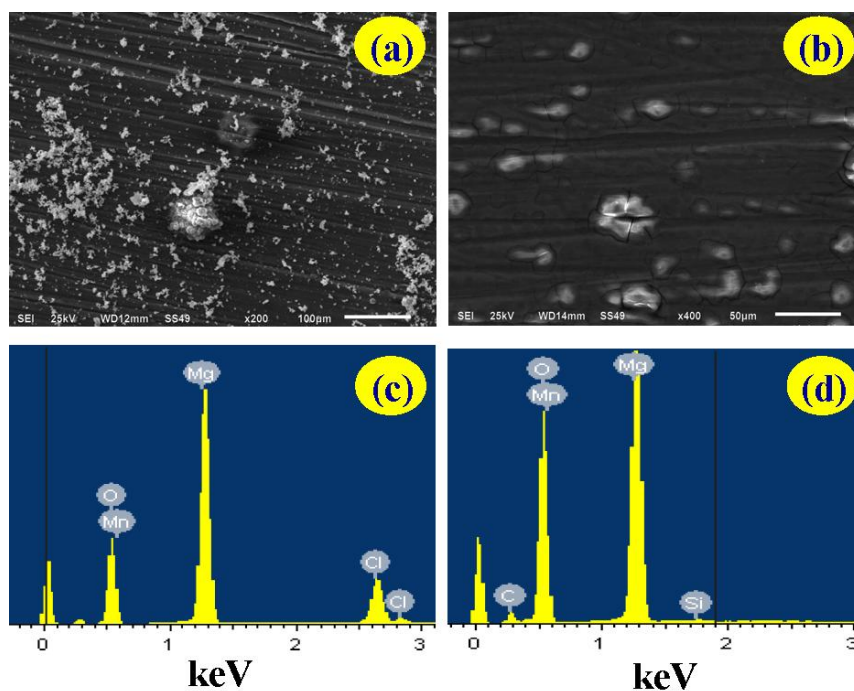
The very low content of Mg indicates that the alloy surface is completely covered with a thick layer of corrosion products. The SEM micrographs for Mg after its immersion for 600 h in 3.5 wt.% NaCl alone, and 3.5 wt.% NaCl + 1×10^{-3} M APTA are shown in Fig. 4a and Fig. 4b and the corresponding EDX profile analysis for the areas shown in these SEM images are shown in Fig. 4c and Fig. 4d, respectively. It is clearly seen from the SEM image (a) of Fig. 4 that there are black and white areas with shaped like pit observed on the Mg surface. The atomic percentage of the elements found on the area shown in the SEM micrograph and displayed in the EDX profile presented in Fig. 4c, were 60.33% O, 33.29% Mg, 6.09% Cl, and 0.29% Mn. This suggests that the compounds formed on the Mg surface are mainly magnesium oxides and some magnesium chlorides. The SEM image obtained on the Mg surface after its immersion in NaCl + 10^{-3} M APTA, Fig. 4b, shows a more homogenous surface that contains a thick and dense layer. The atomic percentage of the elements found in the major investigated surface of the micrograph and represented by the EDX profile shown in Fig. 4d were 60.56% O, 24.00% Mg, 14.96% C, 0.12% Si, and 0.36% Mn. This indicates that the layer formed on the surface mainly contains magnesium oxide in addition to carbon compounds. The high content of carbon compound might have existed due to the adsorption of APTA compound onto Mg during its immersion in the test solution. The absence of chloride from the EDX profile analysis in this area gives more confirmation that the Mg surface is not pitted and well protected by APTA.
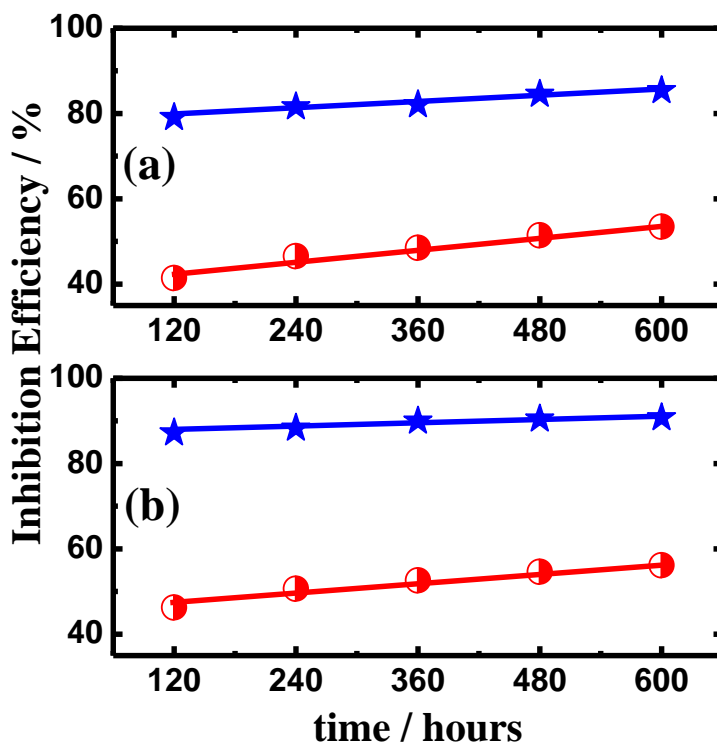

Figure 5. The change of the percentage of inhibition efficiency (IE / %) as a function of time (hour) for Mg coupons in (a) AGS and (b) 3.5 wt.% NaCl solutions that contain (1) 1.0×10^{-3} M APTA, and (2) 5.0×10^{-3} M APTA, respectively.

In order to confirm the ability of APTA molecules on the inhibition of Mg corrosion in AGS and 3.5 wt.% NaCl solutions, the percentage of the inhibition efficiency (IE%) for APTA at $1x10^{-3}$ and $5x10^{-3}$ M APTA was calculated using Eq. (3). Fig. 5 shows the change of the percentage of inhibition efficiency (IE / %) as a function of time (hour) for Mg coupons in (a) AGS and (b) 3.5 wt.% NaCl solutions that contain (1) $1.0x10^{-3}$ M APTA, and (2) $5.0x10^{-3}$ M APTA, respectively. It is seen from Fig. 5a that the addition of $1x10^{-3}$ M APTA to AGS recorded circa 42% after 120 h that was increased with time to record ~ 51% in 600 h. These values highly increased in the presence of $5x10^{-3}$ M APTA to record ~ 80% and 86%, respectively. This effect of APTA on the inhibition of Mg in AGS was almost similar to its effect in 3.5 wt.% NaCl solutions at the same concentration. The only difference was that the values of IE% in NaCl solutions were little higher, where $1x10^{-3}$ M APTA gave about 47% after 120 h increased to about 55% in 600 h. These values also increased with increasing APTA to $5 x10^{-3}$ and recorded 88% and 91%, respectively. This indicates that APTA is a good corrosion inhibitor for Mg in both AGS and NaCl solutions and its inhibition efficiency increases with the increase of its concentration as well as the increase of the exposure time of Mg in the test solutions.

3.2. Potentiodynamic polarization (PDP) measurements
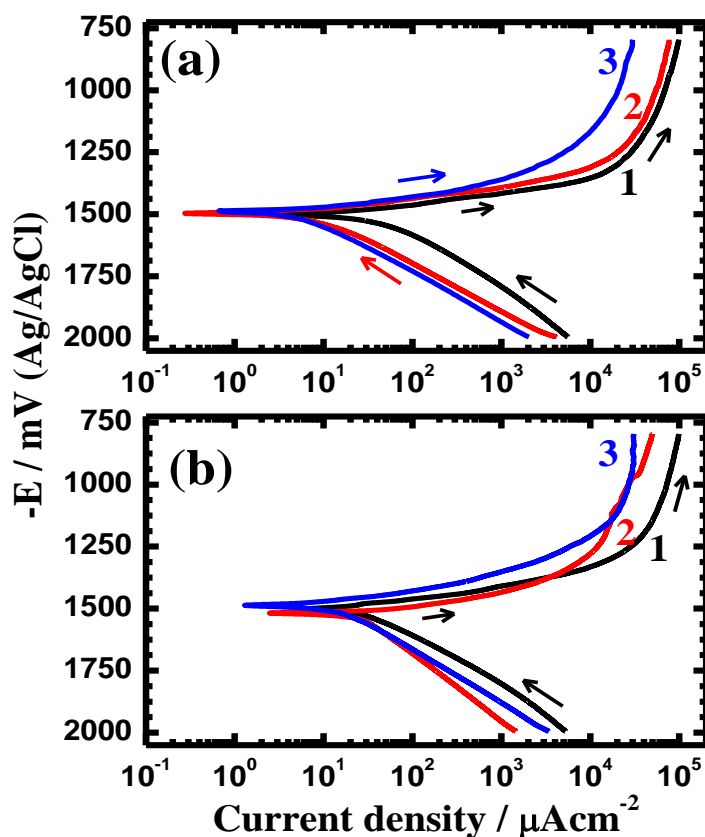

Figure 6. Potentiodynamic polarization curves for Mg electrode after its immersion for 60 min in (a) AGS and (b) 3.5 wt.% NaCl solutions that contain (1) 0.0 M APTA, (2) $1.0x10^{-3}$ M APTA, and (3) $5.0x10^{-3}$ M APTA, respectively.

The PDP curves obtained for Mg after its immersion in (a) AGS and (b) 3.5 wt.% NaCl solutions that contain (1) 0.0 M APTA, (2) 1.0×10^{-3} M APTA, and (3) 5.0×10^{-3} M APTA, respectively are shown in Fig. 6. The values of corrosion potential (E_{Corr}), corrosion current density (j_{Corr}), cathodic (β_c) and anodic (β_a) Tafel slopes, polarization resistance (R_P), and corrosion rate (K_{Corr}) obtained from the PDP curves shown in Fig. 6 are listed in Table 1. All these parameters were obtained and calculated according to our previous studies [47–55]. Fig. 6 shows that an active dissolution occurs for Mg in AGS and 3.5 wt.% NaCl solutions in the absence of APTA (curves 1) with increasing potential in the anodic branch under the aggressiveness action of the chloride ions presented in the test solutions. It is seen from Fig. 6 that the presence of 1×10^{-3} M APTA with AGS and 3.5 wt.% NaCl solutions significantly reduced this Mg dissolution. It is seen also that the increase of APTA concentration to 5×10^{-3} increased that effect and greatly lowered the corrosion of Mg. This is because the presence of APTA and the increase of its concentration remarkably decreased the values of cathodic, j_{Corr} anodic currents and K_{Corr}, and displaced the values of E_{Corr} towards the negative direction as indicated from their listed values in Table 1.

Table 1. Corrosion parameters obtained from potentiodynamic polarization curves shown in Fig. 6 for the Mg electrode in AGS and 3.5 wt.% NaCl solutions without and with APTA.

Solution	Parameter						
	β_c / mV dec^{-1}	E_{Corr} / mV	j_{Corr} / μA cm^{-2}	β_a / mV dec^{-1}	R_p / Ω cm^2	K_{Corr} / mmy^{-1}	IE / %
AGS only	225	−1504	51.0	65	430	1.165	—
+ 1x10-3 M APTA	180	−1528	13.0	68	1651	0.297	74.51
+ 5x10-3 M APTA	180	−1520	7.50	70	2922	0.171	85.32
3.5 wt.% NaCl only	175	−1513	33	63	610	0.754	—
+ 1x10-3 M APTA	255	−1535	15	65	3453	0.343	54.51
+ 5x10-3 M APTA	185	−1495	9	67	5465	0.207	72.54

The negative change of E_{Corr} for Mg in the presence of APTA and upon the increase of its concentration is due to the decrease of the rate of cathodic reactions that occur on Mg surface. The decrease in the values of j_{Corr} and K_{Corr} for Mg is solutions containing APTA resulted from the decrease of the chloride ion attack on the Mg surface, which is also due to the adsorption of APTA molecules on the Mg and prevent the corrosive Cl$^-$ from reaching the surface. This was also confirmed by the increase of R_P values in the presence of APTA and the increase of its content as recorded in Table 1 and indicated also that APTA molecules increase Mg resistance against corrosion. In order to quantify the efficiency of APTA as a corrosion inhibitor for Mg in AGS and 3.5 wt.% NaCl solutions, the values of IE% were calculated as has previously reported [47-50] and listed in Table 1. The increase of IE% with increasing the APTA concentration reveals that APTA has the ability to protect Mg surface against corrosion in AGS and 3.5 wt.% NaCl solutions and its efficiency increases with its concentration. The PDP results thus are in good agreement with the data obtained by weight-loss.

3.3. Chronoamperometric current–time (CT) measurements

In order to shed more light on the ability of APTA molecules on the inhibition of the uniform and pitting corrosion of Mg in AGS and 3.5 wt.% NaCl solutions at an active constant potential value, the CT experiments were carried out . Fig. 7 shows the CT curves obtained at -1200 mV vs. Ag/AgCl for Mg electrode after its immersion for 60 min in (a) AGS and (b) 3.5 wt.% NaCl solutions that contain (1) 0.0 M APTA, (2) 1.0×10^{-3} M APTA, and (3) 5.0×10^{-3} M APTA, respectively. This potential value, -1200 mV, was determined from polarization curves. It is seen from Fig. 7 that the currents of Mg in AGS and 3.5 wt.% NaCl solutions without APTA present, curves 1, showed a rapid increase in the first few moments due to the dissolution of an air formed magnesium oxide film. The current then slowly decreased and increased with fluctuations in its values up to the end of the run. The current values and the appearance of current fluctuations indicate that Mg surfers both pitting and uniform corrosion at this condition [56-58].
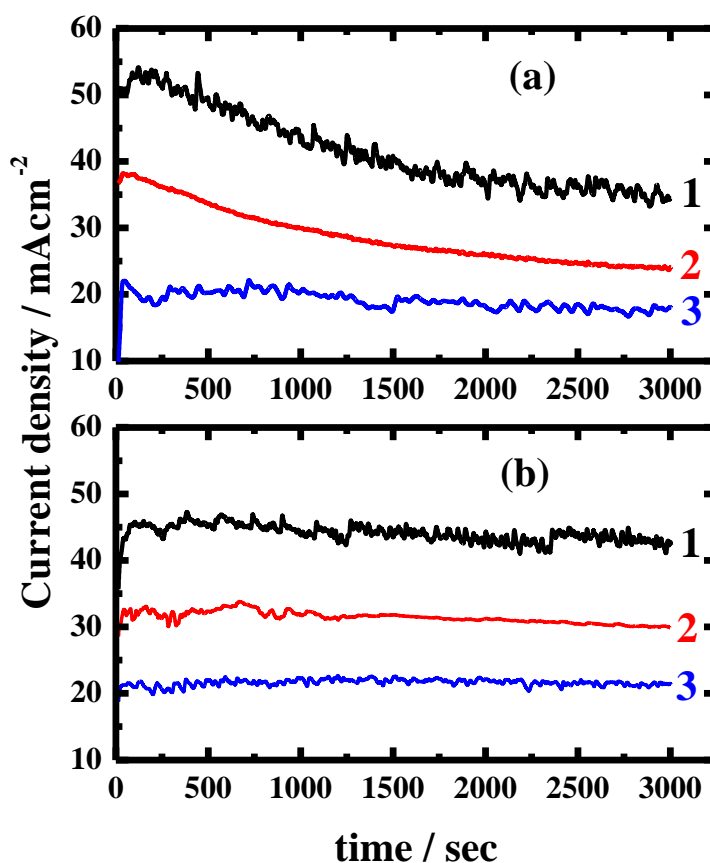

Figure 7. Chronoamperometric current-time curves at -1200 mV vs. Ag/AgCl for Mg electrode after its immersion for 60 min in (a) AGS and (b) 3.5 wt.% NaCl solutions that contain (1) 0.0 M APTA, (2) 1.0×10^{-3} M APTA, and (3) 5.0×10^{-3} M APTA, respectively.

It has been reported that, the pits develop at sites where oxygen adsorbed on the metal surface is displaced by an aggressive species such as Cl^{-} ions that already present in test media. This is

because Cl⁻ ions have smaller diameter than oxygen, which allows it to penetrate through the oxide film and displace oxygen at the sites where metal-oxygen bond is the weakest [59].

On the other hand, the presence of 1.0×10^{-3} M APTA (Fig. 7, curves 2) largely decreased the absolute current values and the current fluctuations with time. This results from the fact that the adsorption of APTA molecules on Mg increased its surface compactness, which in turn increased the Mg surface resistance against chloride ions attack. This effect was found to increase with increasing the APTA concentration to 5.0×10^{-3} as can be seen from curves 3 of Fig. 7. The CT measurements thus provide another prove that APTA is a powerful corrosion inhibitor against Mg uniform and pitting corrosion in AGS and 3.5 wt.% NaCl solutions and its effectiveness increases with the increase of its concentration. This also agrees with the obtained data by weight-loss and PDP measurements.

3.4. Electrochemical impedance spectroscopy (EIS) measurements

Fig. 8 shows the Nyquist plots obtained for Mg at an OCP after its immersion for 60 min in (a) AGS and (b) 3.5 wt.% NaCl solutions that contain (1) 0.0 M APTA, (2) 1.0×10^{-3} M APTA, and (3) 5.0×10^{-3} M APTA, respectively.
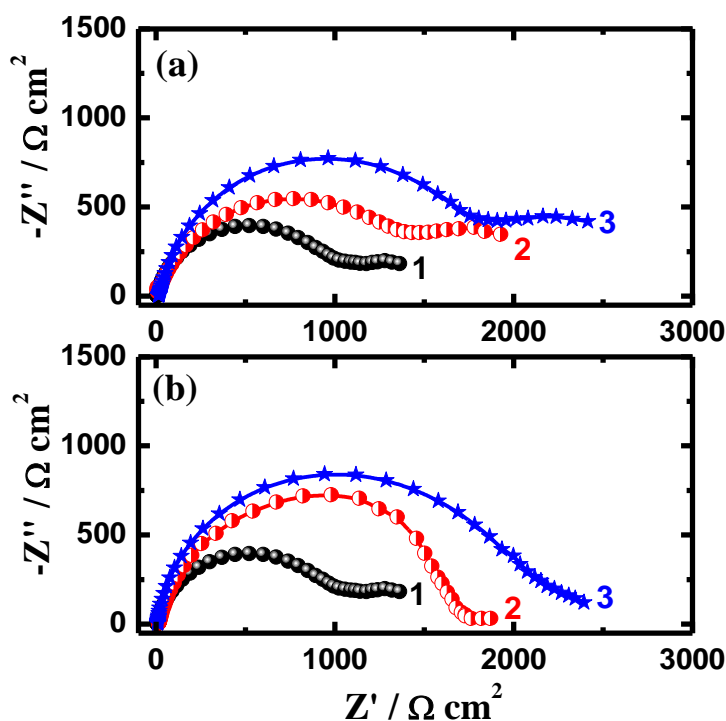

Figure 8. Typical Nyquist plots taken at the corrosion potential for Mg electrode after its immersion for 60 min in (a) AGS and (b) 3.5 wt.% NaCl solutions that contain (1) 0.0 M APTA, (2) 1.0×10^{-3} M APTA, and (3) 5.0×10^{-3} M APTA, respectively.

The measured values of the EIS spectra were analysed by fitting to the equivalent circuit model shown in Fig. 9. The EIS parameters obtained from the equivalent circuit, in addition to the calculated

values of IE% are listed in Table 2. The values of IE% obtained from EIS spectra were calculated as has been reported in our previous studies [21,24]. According to usual convention, R_S represents the solution resistance between Mg and the counter (platinum) electrode, Q_1 and Q_2 the constant phase elements (CPEs), R_{P1} the resistance of a film layer formed on the surface of Mg, and R_{P2} accounts for the polarization resistance at the Mg surface.

It is clearly seen from Fig. 8 that the diameter of the semicircle obtained for in AGS and NaCl solutions in the absence of the inhibitor recorded the lowest size. The diameters then greatly increased in the presence of 1×10^{-3} M APTA molecules and further with the increase of APTA concentration to 5×10^{-3} M. It is seen also form Table 2 that the presence of APTA and the increase of its concentration increased the values of R_S, R_{P1} and R_{P2}. The higher the sum of the polarization resistances, $R_{P1} + R_{P2}$, the stronger is the resistance of Mg against uniform corrosion rate. This is opposed to the tendency towards pitting corrosion. The CPEs, Q_1 and Q_2 with their n values go to 1.0 represent double layer capacitors with some pores; the CPE reported here can be defined as follows [60],

$$Z(CPE) = \left(\frac{Y_0 - 1}{(j\omega)^n} \right) \qquad (8)$$

Where, Y0 is the CPE constant, ω is the angular frequency (in rad s^{-1}), $j^2 = -1$ is the imaginary number and n is the CPE exponent. Depending on the value of n, CPE can represent resistance (Z(CPE) = R, n = 0), capacitance (Z(CPE) = C, n = 1) or Warburg impedance for (n = 0.5). The values of n, especially in APTA containing solutions, indicate that the constant phase elements represent a capacitor but not pure due to the heterogeneity or the presence of some porosity in the formed layer on the Mg surface.
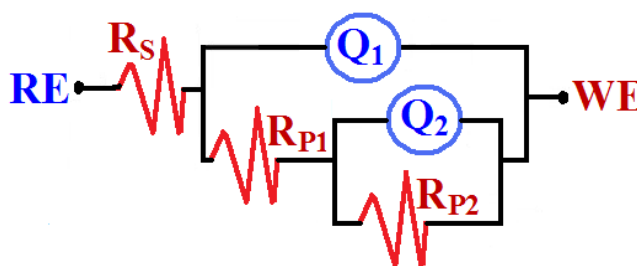

Figure 9. Equivalent circuit model used to fit the EIS Nyquist plots presented in Fig. 8.

The CPEs decrease upon addition and the increase of APTA concentration, where the capacitive effects decrease due to the presence of APTA layers with $Mg(OH)_2$, Eq. (5) and MgO, Eq. (8), on the Mg surface. The increase of IE% of APTA with the increase of its concentration form 1.0×10^{-3} to 5.0×10^{-3} M indicates also that APTA has increased ability to protect Mg against corrosion in AGS and 3.5 wt.% NaCl solutions. The impedance data therefore agree with those ones obtained by weight-loss, PDP and CT, all confirm that APTA decreases the both the uniform and pitting corrosion of Mg in the tested solutions.

Table 2. Impedance parameters obtained by fitting the Nyquist plots shown in Fig. 8 with the equivalent circuit shown in Fig. 9 for magnesium electrodes after immersion in AGS and 3.5 wt.% NaCl solutions in the absence and presence of APTA.

Solution	Parameter								
	R_S / Ωcm^2	Q_1			R_{P1} / $\Omega\ cm^2$	Q_2			R_{P2} / $\Omega\ cm^2$	IE / %
		Y_{Q1} / $\mu F\ cm^{-2}$	n		Y_{Q2} / $\mu F\ cm^{-2}$	n		
AGS only	6.425	20.49	0.89	289	10.6	0.11	551	—
+ $1x10^{-3}$ M APTA	12.13	0.53	1.00	940	6.97	0.79	1659	67.68
+ $5x10^{-3}$ M APTA	19.02	0.47	1.00	1520	0.45	0.85	2128	76.97
3.5 wt.% NaCl only	8.420	0.205	0.80	320	1.058	0.11	629	—
+ $1x10^{-3}$ M APTA	11.34	0.145	0.89	970	0.766	0.86	1746	65.06
+ $5x10^{-3}$ M APTA	17.10	0.086	1.00	1161	0.339	0.93	2127	71.14

4. CONCLUSIONS

The corrosion inhibition of Mg Arabian Gulf seawater (AGS) and 3.5 wt.% NaCl solutions by 5-(3-aminophenyl)-tetrazole (APTA) was studied. Conventional weight-loss, potentiodynamic polarization (PDP), chronoamperometric current-time (CT) measurements and electrochemical impedance spectroscopy (EIS) along with SEM and EDX investigations were used. Weight-loss measurements revealed that the dissolution of Mg increases in AGS and NaCl solutions with increasing time and the presence of APTA and the increase of its concentrations greatly decreases Mg corrosion. SEM micrographs and EDX profile analyses for Mg after 600 h immersion in AGS and NaCl solutions without and with APTA molecules indicated that the uniform and pitting corrosion take place on the Mg surface; this effect decreases in the presence of 10^{-3} M APTA. Only Mg in AGS alone shows a possibility of having microbial induced corrosion repersented by mushroom like corrosion products. PDP and CT experiments confirmed that the presence of APTA and the increase of its content decreases both the uniform and pitting corrosion by decreasing the corrosion current and corrosion rate and increasing the polarization resistance. EIS spectra showed an increased surface and polarizations resistances for Mg with APTA concentration. Experiments together proved clearly that Mg shows a significant uniform and pitting corrosion in AGS and 3.5 wt.% NaCl solutions, while the presence of APTA and the increase of its concentration greatly prevent this Mg corrosion via APTA molecules adsorption onto its surface.

References

1. El-Sayed M. Sherif, A.A. Almajid, *Int. J. Electrochem. Sci.*, 6 (2011) 2131.

2. M. Hakamada, T. Furuta, Y. Chino, Y.Q. Chen, H. Kusuda, M. Mabuchi, *Energy,* 32 (2007) 1352.
3. El-Sayed M. Sherif, Int. J. Electrochem. Sci., 6 (2011) 5372.
4. M.P. Staiger, A.M. Pietak, J. Huadmai, G. Dias, *Biomaterials,* 27 (2006) 1728.
5. Sebastián Feliu Jr., C. Maffiotte, Alejandro Samaniego, Juan Carlos Galván, Violeta Barranco, *Electrochim. Acta*, 56 (2011) 4554.
6. X. Cao, M. Jahazi, J.P. Immarigeon, W. Wallace, *J. Mater. Pro. Technol.,* 171 (2006) 188.
7. A.R. Shashikala, R. Umarani, S.M. Mayanna, A.K. Sharma, *Int. J. Electrochem.* Sci., 3 (2008) 993.
8. Reidar Tunold, Hans Holtan, May-Britt Hägg Berge, Axel Lasson, Rolf Steen-Hansen, *Corros. Sci.,* 17 (1977) 353.
9. G. Song, A. Atrens, D.St John, X. Wu, J. Nairn, *Corros. Sci.,* 39 (1997) 1981.
10. H. Inoue, K. Sugahara, A. Yamamoto, H. Tsubakino, *Corros. Sci.,* 44 (2002) 603.
11. El-Sayed M. Sherif, *Int. J. Electrochem. Sci*., 7 (2012) 4235.
12. Geraint Williams, H. Neil McMurray, *J. Electrochem. Soc.,* 155 (2008) C340.
13. Guangling Song, Andrej Atrens, *Adv. Eng. Mater.,* 5 (2003) 837.
14. Andrej Atrens, Nicholas Winzer, Wolfgang Dietzel, *Adv. Eng. Mater*., 13 (2011) 11.
15. G. Song, A. Atrens, *Adv. Eng. Mater.,* 1 (1999) 11.
16. G.T. Parthiban, K. Bharanidharan, D. Dhayanand, Thirumalai Parthiban, N. Palaniswamy, V. Sivan, *Int. J. Electrochem. Sci.,* 3 (2008) 1162.
17. Guangling Song, *Adv. Eng. Mater.,* 7 (2005) 563.
18. Anna Da Forno, Massimiliano Bestetti, *Adv. Res. Mater.*, 138 (2010) 79.
19. J. Kim, K.C. Wong, P.C. Wong, S.A. Kulinich, J.B. Metson, K.A.R. Mitchell, *Appl. Surf. Sci.,* 253 (2007) 4197.
20. El-Sayed M. Sherif, *Int. J. Electrochem. Sci.,* 7 (2012) 2832.
21. E. M. Sherif, S.-M. Park, *Corros. Sci.,* 48 (2006) 4065.
22. El-Sayed M. Sherif, A.A. Almajid, *J. Appl. Electrochem.,* 40 (2010) 1555.
23. El-Sayed M. Sherif, *Int. J. Electrochem. Sci.* 6 (2011) 1479.
24. El-Sayed M. Sherif, R.M. Erasmus, J.D. Comins, *Electrochim. Acta,* 55 (2010) 3657.
25. El-Sayed M. Sherif, *J. Mater. Eng. Performance,* 19 (2010) 873.
26. El-Sayed M. Sherif, A.H. Ahmed, *Synthesis and Reactivity in Inorganic, Metal-Organic, and Nano-Metal Chemistry*, 40 (2010) 365.
27. El-Sayed M. Sherif, *Int. J. Electrochem. Sci.*, 6 (2011) 3077.
28. El-Sayed M. Sherif, *Int. J. Electrochem. Sci.*, 7 (2012) 1482.
29. El-Sayed M. Sherif, R.M. Erasmus, J.D. Comins, *J. Appl. Electrochem*., 39 (2009) 83.
30. El-Sayed M. Sherif, *J. Appl. Surf. Sci*., 252 (2006) 8615.
31. E.M. Sherif, S.-M. Park, *J. Electrochem. Soc*., 152 (2005) B428.
32. E.M. Sherif, S.-M. Park, *Electrochim. Acta*, 51 (2006) 1313.
33. G. Williams, H.N. McMurray, R. Grace, *Electrochim. Acta*, 55 (2010) 7824.
34. Xu Yang, Fu Sheng Pan, Ding Fei Zhang, *Mater. Sci. Forum,* 610-613 (2009) 920.
35. Yair Tamar, Daniel Mandler, *Electrochim. Acta*, 53 (2010) 5118.
36. El-Sayed M. Sherif, R.M. Erasmus, J.D .Comins, *J. Appl. Electrochem.,* 39 (2009) 83.
37. El-Sayed M. Sherif, R.M. Erasmus, J.D. *Comins, Corros. Sci.,* 50 (2008) 3439.
38. El-Sayed M. Sherif, *Mater. Chem. Phys*., 129 (2011) 961.
39. El-Sayed M. Sherif, R.M. Erasmus, J.D. Comins, *J. Colloid Interface Sci*., 309 (2007) 470.
40. El-Sayed M. Sherif, J.H. Potgieter, J.D. Comins, L. Cornish, P.A. Olubambi, C.N. Machio, *Corros. Sci*., 51 (2009) 1364.
41. El-Sayed M. Sherif, *J. Solid State Electrochem.,* 16 (2012) 891.
42. El-Sayed M. Sherif, *Int. J. Electrochem. Sci.,* 7 (2012) 1884.
43. El-Sayed M. Sherif, *Int. J. Electrochem. Sci.,* 7 (2012) 2374.
44. Zhiming Shi, Andrej Atrens, *Corros. Sci.,* 53 (2011) 226.
45. S. Bender, J. Goellner, A. Heyn, E. Boese, *Mater. Corros.,* 58 (2007) 977.

46. A.Pardo, M.C. Merino, A.E. Coy, R. Arrabal, F. Viejo, E. Matykina, *Corros. Sci.,* 50 (2008) 823.
47. El-Sayed M. Sherif, J. H. Potgieter, J. D. Comins, L. Cornish, P. A. Olubambi, C. N. Machio, J. Appl. Electrochem. 39 (2009) 1385.
48. E.M. Sherif, S.-M. Park, Electrochim. Acta 51 (2006) 4665.
49. Khalil A. Khalil, El-Sayed M. Sherif, A.A. Almajid, *Int. J. Electrochem. Sci.,* 6 (2011) 6184.
50. El-Sayed M. Sherif, *Int. J. Electrochem. Sci*., 6 (2011) 2284.
51. El-Sayed M. Sherif, A.A. Almajid, A.K. Bairamov, Eissa Al-Zahrani, *Int. J. Electrochem. Sci.,* 6 (2011) 5430.
52. El-Sayed M. Sherif, A.A. Almajid, A.K. Bairamov, Eissa Al-Zahrani, *Int. J. Electrochem. Sci.,* 7 (2012) 2796.
53. F.H. Latief, El-Sayed M. Sherif, A.A. Almajid, H. Junaedi, *J. Anal. Appl. Pyrolysis,* 92 (2011) 485.
54. El-Sayed M. Sherif, A.A. Almajid, F.H. Latif, H. Junaedi, *Int. J. Electrochem. Sci.,* 6 (2011) 1085
55. A.A. El Warraky, H.A. El Shayeb, E.M. Sherif, *Anti-Corros. Methods Mater.,* 51 (2004) 52.
56. El-Sayed M. Sherif, E.A. El-Danaf, M.S. Soliman, A.A. Almajid, *Int. J. Electrochem. Sci.,* 7 (2012) 2846.
57. E.M. Sherif, S.-M. Park, *Electrochim. Acta,* 51 (2006) 6556.
58. E.M. Sherif, S.-M. Park, *J. Electrochem. Soc*., 152 (2005) B205.
59. Z. Szklarska-Smialowska, Editor, *Pitting Corrosion of Metals,* NACE International, Houston (1986).
60. Z. Zhang, S. Chen, Y. Li, S. Li, L. Wang, *Corros. Sci.,* 51 (2009) 291.